Modeling Interband Transitions in Silver Nanoparticle−Fluoropolymer Composites

Kevin C. See,[†] James B. Spicer,*[,†] John Brupbacher,[‡] Dajie Zhang,[‡] and Terrence G. Vargo[§]

Department of Materials Science and Engineering, Johns Hopkins University, Baltimore, Maryland 21218-2681; Center for Multi-Functional Appliqué, Johns Hopkins University, Baltimore, Maryland 21211-2806; and Integument Technologies, Inc., Tonawanda, New York 14150-6711

Received: July 26, 2004; In Final Form: October 14, 2004

The interband transition contributions to the optical properties of silver nanoparticles in fluoropolymer matrices are investigated. For the materials in this study, nanoparticle synthesis within the existing polymer matrix is accomplished using an infusion process that consists of diffusing an organometallic precursor gas into the free volume of the fluoropolymer and decomposing the precursor followed by metal nanoparticle nucleation and growth. The resulting polymer matrix nanocomposite has optical properties that are dominated by the response of the nanoparticles owing to the broadbanded transparency of the fluoropolymer matrix. The optical properties of these composites are compared to Maxwell−Garnett and Mie theory with results indicating that interband transitions excited in the silver nanoparticles affect the optical absorption over a range of frequencies including the surface plasmon resonance. It is shown that calculations of the optical absorption spectrum using published data for the silver dielectric function do not accurately describe the measured material response and that a classical model for bound and free electron behavior can best be used to represent the dielectric function of silver.

1. Introduction

The optical properties of metallic nanoparticles differ greatly from the corresponding bulk metal. As particle size decreases, the conduction electrons begin to interact with the boundary of the particle.[1] Displacement of conduction electrons with respect to the positive ionic background following irradiation by electromagnetic waves induces surface polarization charges that result in a linear restoring force. At appropriate frequencies this linear restoring force gives rise to a characteristic oscillation known as a surface plasmon.[2] This oscillation is often known as the surface plasmon resonance (SPR).

The SPR phenomenon is most obviously manifested in a peak in the optical absorption spectrum of nanoparticles with the surrounding medium affecting the frequency of the SPR.[3] Certain noble metals, specifically gold and silver, exhibit SPR absorption peaks in the visible portion of the spectrum that result in unique colors differing from the bulk. The prominence of the SPR in noble metal nanoparticles has enabled investigations into biosensing applications using the characteristics of gold and silver nanoparticle systems.[4,5] Because of these characteristics, silver systems have been particularly popular for a variety of studies.

The optical absorption of a metal relies exclusively on its dielectric function. In modeling the absorption of metal nanoparticles, the selection of the appropriate dielectric function is crucial. In some cases, researchers have utilized a damped Drude model that considers a free electron metal with damping.[6] However, it is well-known that bulk silver not only displays free electron behavior but also exhibits bound electron effects related to interband transitions that are classically modeled using Lorentz oscillators.[1,7,8] Even though the dielectric function has been measured and well characterized for a number of systems, there is evidence of deviation between bulk values extracted from measurements on thin films[9] and measurements on nanoparticle populations.[10] This indicates that the effective dielectric function of silver varies depending on the size and environment of the silver.

In this work, a system of silver nanoparticles residing in a fluoropolymer matrix was studied to determine the optical behaviors of the composite as well as the nanoparticles. Samples were synthesized by first infusing an organometallic precursor species into a solid polymer matrix followed by thermal decomposition of the precursor along with nucleation and growth of metal particles in the polymer. An organic byproduct was also created and was subsequently removed by evacuation. The resulting composite of nanoparticles inside the fluoropolymer matrix represents a particularly robust, stable material system owing to the physical and chemical properties of the matrix. The infusion process allows for the synthesis of a variety of nanoparticles within preformed polymeric particles, films, or sheets while maintaining the overall structure of the polymer.[11] Measured ultraviolet−visible absorption spectra for these nanocomposites display peaks in the ultraviolet that have not been investigated thoroughly. The measured peaks have a larger magnitude and are better defined than are those calculated using Mie theory based on previously measured values for the silver dielectric function.[9,10] This indicates that the dielectric function for silver required to model our material differs significantly from previous work. The goal of this study is to model the optical absorption spectrum of silver−fluoropolymer nanocomposites considering both damped, free electron and interband transition contributions to the dielectric function of these materials.

[†] Department of Materials Science and Engineering, Johns Hopkins University.
[‡] Center for Multi-Functional Appliqué, Johns Hopkins University.
[§] Integument Technologies, Inc.
* Corresponding author: E-mail: spicer@jhu.edu; phone: 410-516-8524; fax: 410-516-5293.

10.1021/jp046687h CCC: $30.25
Published on Web 02/02/2005

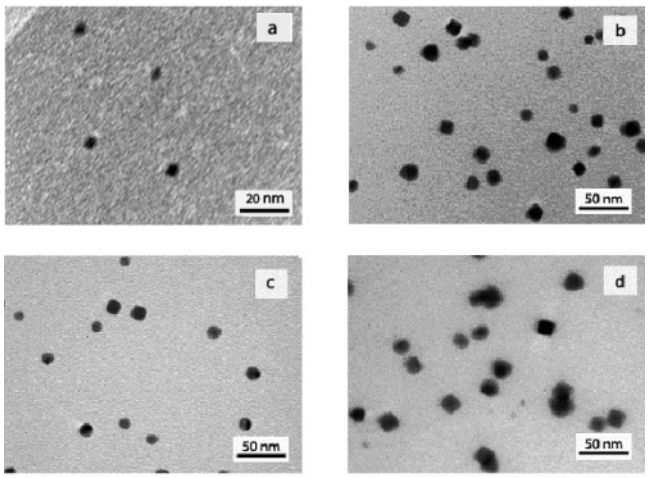

Figure 1. Transmission electron microscope images of silver−FEP nanocomposites: (a) 1×, (b) 5×, (c) 10×, and (d) 16× infusion cycles.

2. Material System

Nanocomposite Synthesis. The material system used in the current study is a nanocomposite composed of a hexafluoropropylene-*co*-tetrafluoroethylene (FEP) matrix with embedded silver nanoparticles. The particles were fabricated in situ after infusion of the organometallic precursor vinyltriethylsilane-(hexafluoroacetylacetonate)silver(I) [$Ag(CF_3COCHCOCF_3)(C_8H_{18}Si)$] into a 250 μm thick FEP film followed by thermal decomposition of the precursor. To synthesize the composite, the polymer matrix is placed in a glass reactor vessel along with the liquid precursor. The precursor is frozen by immersing the vessel in a shallow dewar of liquid nitrogen. It is subsequently evacuated below 30 Torr using a mechanical roughing pump. Following evacuation, the vessel is closed and the precursor is allowed to thaw and outgas to reduce impurities. This freezing/evacuation/thawing process is repeated until sufficient precursor purity is obtained. Following the final evacuation and with the vessel still under vacuum, the vessel is placed in a furnace at 90 °C for 1 h, enabling the vaporization and infusion of the precursor into the polymer. The temperature is then raised to 160 °C for 12 h to decompose the precursor into its constituent metallic and organic components. Finally, the vessel is evacuated once more to remove the organic decomposition product. This infusion process can be repeated consecutively to produce samples with varying amounts of silver content. For convenience, the samples are denoted by the number of infusions performed (e.g., 1×, 3×, 5×, etc.) in synthesizing the composite.

Material Characteristics. The infusion process appears to depend on the amorphous/crystalline structure of the polymer and can be carried out for materials with precursor chemical species that can be vaporized and decomposed below the melting temperature of the polymer matrix. Preliminary studies have shown that the highest possible content of nanoparticles in various nanocomposite systems has been achieved in semicrystalline polymer matrices, indicating a heterogeneous nucleation mechanism. Further study is underway to understand the nature of particle nucleation and growth inside the polymer.

TEM images of various silver−FEP materials are shown in Figure 1. Weight percentages were determined by mass measurements before and after final processing. By assuming bulk density of silver for the nanoparticles, the volume percentage of silver in each sample can be determined and is shown in Figure 2 along with the corresponding weight percentages. The

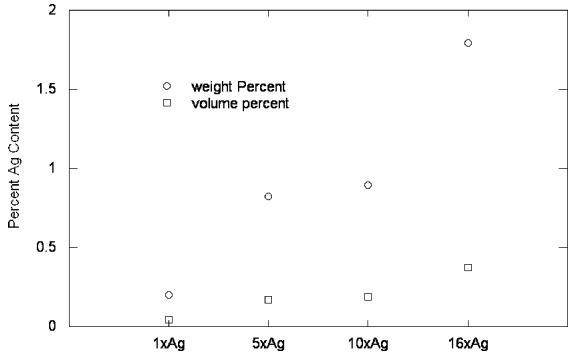

Figure 2. Silver content for each silver−FEP nanocomposite as a function of the number of infusion cycles.

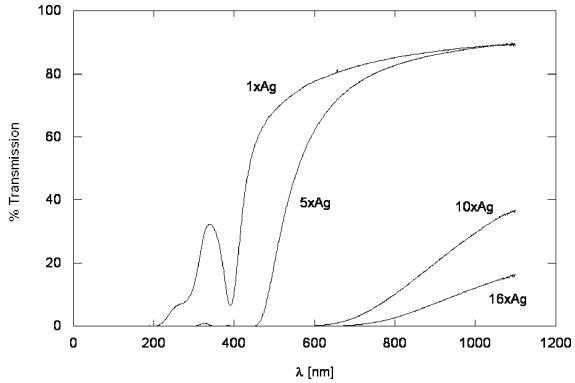

Figure 3. Total optical transmission spectra for silver−FEP nanocomposites as a function of the number of infusion cycles performed during material processing.

samples produced have low silver content with the highest being only 0.37 vol %.

The films are transparent and appear to have homogeneous optical transmission characteristics across the width and height of each sample. Aspects of the optical properties are given by the optical transmission spectra shown in Figure 3 for the 1×, 5×, 10×, and 16× nanocomposites.

The spectra for the 1× and 5× nanocomposites show transmission minima near 392 nm, corresponding to the SPR for these materials. Overall, the 1× and 5× materials are clear and appear to be yellow as a result of the strong SPR absorption in the blue. The optical attenuation is so large for the other materials that no clearly defined SPR can be inferred from the transmission spectra. However, microscopic examinations of the 10× and 16× materials show that the polymers containing the most silver appear to be a very dark red. This result is consistent with studies that show the color of embedded silver nanoparticles undergo a transition from yellow to red with increasing particle size.[12]

To further understand the character of the silver nanoparticles and to aid the interpretation of the measured optical properties, X-ray diffraction measurements were made to assess the crystallinity of the particles. The corresponding results are shown in Figure 4 for the 16× material. The diffraction from the uninfused polymer was also measured so that scaling and subtracting the matrix contribution could be performed to isolate effects due to the nanoparticles. There are diffraction peaks related to the particles that appear at locations corresponding to those for bulk silver. The broadening of the peaks is consistent with diffraction scans of nanoparticles and can be attributed primarily to particle size.[13,14] For the 16× material, analysis of

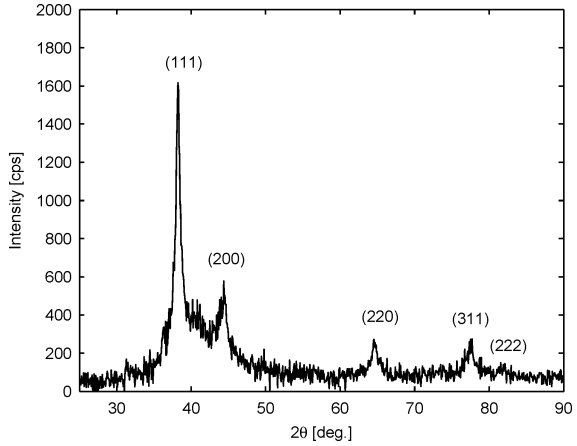

Figure 4. X-ray diffraction pattern of silver nanoparticles in a FEP matrix. The background contributions from the matrix have been subtracted to show only those features related to the nanoparticles in the composite. Peak assignments to silver crystal planes are shown for each peak.

the peaks yields a particle size between 12 and 13 nm, in good agreement with the TEM micrographs in Figure 1. These results imply that the particles are crystalline and support the use of the bulk density values for silver to calculate volume fractions.

3. Modeling Nanoparticle Absorption

Modeling efforts have been carried out to aid the understanding of the optical properties of these composites. One method of modeling the absorption properties of nanoparticle systems involves the approximation of a small particle/matrix composite as a homogeneous effective medium. This effective medium approach attempts to define an average or effective dielectric function for the material system.[1,2] Here we use the Maxwell−Garnett model to define an average dielectric function for the material. This model assumes that there are homogeneous electromagnetic fields within and outside the particle as well as a low filling factor for particles in the composite. The latter requirement is important because it allows us to assume dipole excitations only and is satisfied for our composites based on volume percentage calculations along with the results shown in the TEM images. The Maxwell−Garnett effective dielectric function is given by

$$\epsilon_{\text{eff}} = \epsilon_{\text{m}}\left[1 + \frac{3f\left(\frac{\epsilon - \epsilon_{\text{m}}}{\epsilon + 2\epsilon_{\text{m}}}\right)}{1 - f\left(\frac{\epsilon - \epsilon_{\text{m}}}{\epsilon + 2\epsilon_{\text{m}}}\right)}\right] \tag{1}$$

where ϵ_{m} is the dielectric constant of the polymer matrix, $\epsilon = \epsilon_1 + i\epsilon_2$ is the dielectric function of the metal particle, and f is the filling factor of particles. The spectrometer measures the transmission of the radiation through the material, and consequently, the experimental results relate to the extinction of the system, i.e., the sum of absorption and scattering intensities. In the case where particles are sufficiently small compared to the wavelength of incident irradiation, it is well-known that absorption contributions greatly exceed scattering contributions.[2,15] Again, TEM results show that the 1× composite sample satisfies this requirement, and we are able to refer to the extinction coefficient as the absorption coefficient since extinction is dominated by absorption. The absorption coefficient is given by

$$\mu = \frac{2\omega}{c}\left[-\frac{\epsilon_{1,\text{eff}}}{2} + \frac{\sqrt{\epsilon_{1,\text{eff}}^2 + \epsilon_{2,\text{eff}}^2}}{2}\right]^{1/2} \tag{2}$$

where c is the speed of light, ω is the frequency of incident light, and $\epsilon_{\text{eff}} = \epsilon_{1,\text{eff}} + i\epsilon_{2,\text{eff}}$.

Since we know the filling fraction for the 1× composite sample is very low, we can use a simpler approximate form of the absorption coefficient given in eq 2. Ruppin showed that, by power series expansion of eq 2 and keeping the lowest order term in f, absorption can be expressed as

$$\mu = 9f\frac{\omega}{c}\epsilon_{\text{m}}^{3/2}\frac{\epsilon_2}{(\epsilon_1 + 2\epsilon_{\text{m}})^2 + \epsilon_2^2} \tag{3}$$

which is the same result obtained from Mie theory in the quasi-static approximation.[16,17]

As discussed earlier, the critical step is the selection of the appropriate dielectric function for the silver particles. Most metals are predominantly characterized by free electron behavior and have a dielectric function of the Drude form:

$$\epsilon_{\text{f}} = 1 - \frac{\omega_{\text{p}}^2}{\omega^2 + i\gamma\omega} \tag{4}$$

where the f denotes free electron contributions, ω_{p} is the plasma frequency of the metal, ω is the frequency of incident radiation, and γ is the phenomenological damping constant. ω_{p} is defined as

$$\omega_{\text{p}} = \sqrt{\frac{Ne^2}{m\epsilon_0}} \tag{5}$$

where N, e, m, and ϵ_0 are the number density of electrons, charge of an electron, electron effective mass, and permittivity of free space, respectively. It has been shown that the bulk dielectric function for metals is applicable for nanoparticles by introducing an altered damping constant that incorporates size effects.[2,18] As the particle size approaches the mean free path of the bulk metal, scattering at the particle surface becomes important and is modeled by modifying the damping constant and making it a function of particle size.[1,2] This damping function is defined as

$$\gamma = \gamma_{\text{b}} + A\frac{\nu_{\text{f}}}{r} \tag{6}$$

where the bulk damping constant $\gamma_{\text{b}} = \nu_{\text{f}}/l_{\text{b}}$, $\nu_{\text{f}} = 1.39 \times 10^{15}$ nm/s is the Fermi velocity of silver,[19] $l_{\text{b}} = 52$ nm is the bulk mean free path of silver,[2] and r is the particle radius. For this description, A is a parameter that takes into account both quantum size effects along with particle−matrix interface effects.[18,20,21] It contains information on the scattering processes involved during optical excitation and relates to the width of the SPR.

Figure 5 shows the optical absorption spectrum for the 1× composite from 225 to 600 nm obtained using the results shown in Figure 3. Here the background absorption of the matrix has been eliminated to isolate the matrix-dependent properties of the silver nanoparticles. The most prominent feature in this spectrum is the well-known plasmon resonance that occurs at ∼392 nm. In addition, there are well-defined features that extend

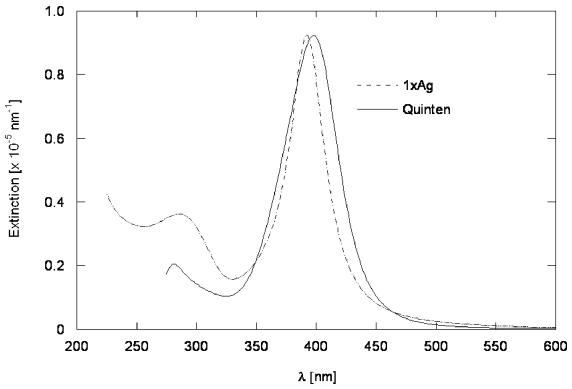

Figure 5. Experimentally measured absorption spectrum for the 1× silver nanocomposite shown with a calculated, best fit spectrum using the dielectric function of silver from ref 10 along with eqs 4 and 6. Values were $r = 5$ nm, $\epsilon_m = 1.68$, $f = 3.80 \times 10^{-5}$, and $A = 0.26$.

from the plasmon resonance down to ~200 nm. We believe these are manifestations of interband contributions to the dielectric function of our metal particles. For comparison, the bulk dielectric function of silver extracted from measurements on chemically prepared silver clusters[10] was used to calculate absorption using eq 3. The bulk data were adjusted for particle size using the procedure originally outlined by Kreibig and Fragstein using eqs 4 and 6.[22] The only variables used to fit the bulk data to our results were the particle size, dielectric constant of the matrix ϵ_m, the filling factor *f*, and the *A* parameter. The particle size was restricted to radii between 1 and 5 nm based on the TEM images of the 1× and 3× samples. Five least-squares analyses were run, fixing the radius between 1 and 5 nm for each and letting *f*, *A*, and ϵ_m vary. The best fit is shown in Figure 5.

Two major observations come from this comparison. First, the calculated SPR resides at the correct position, but the width of the peak exceeds that of the measurement. The peak width is narrowest for the parameters selected and would be wider for the smaller particles that are in our 1× material. Second, even though the bulk silver data do yield a peak in the 280 nm range, the absorption at wavelengths below ~350 nm (at the onset of interband transitions) differs considerably. Both observations point to the possibility that the dielectric function of the silver in our 1× material differs from the bulk dielectric function of silver extracted from systems with larger particles. This is the case for Quinten's silver particles which ranged from 16.6 to 32 nm in diameter. Finally, it should be noted that the Quinten data do not extend to wavelengths below 275 nm where there is still considerable information about the silver particles in our composite. Since it was not possible to reproduce the absorption spectrum using published values for silver, it appears that the dielectric function for the particles in our 1× composite differs from that in this previous report.[10]

Similarly, previously published values[9] for the dielectric function of silver were unable to reproduce absorption spectra of our particles. It should be emphasized that the peak width could not be reproduced using common assumptions regarding the damping constant and the *A* parameter.[3,23] Perhaps the simplest explanation relates directly to interband behavior of silver since increased interband transition contributions have been shown to result in a narrower SPR peak. The mechanism of this narrowing relates to increases in the derivative $d\epsilon_1(\omega)/d\omega$ which narrow the plasmon peak.[2,3,13] Given the shortcomings of published data on the silver dielectric constant, we will concentrate on modeling the contributions of interband transitions.

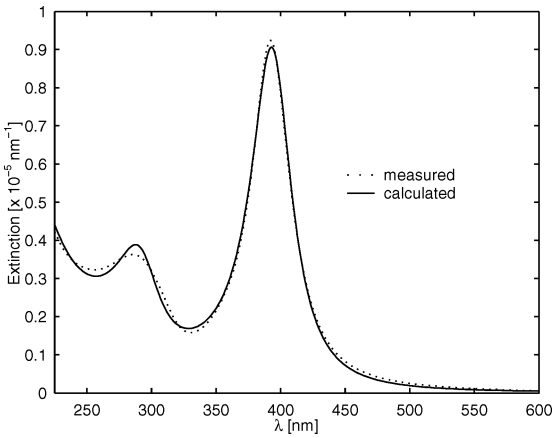

Figure 6. Absorption spectrum of 1× silver−FEP nanocomposite with best fit of eq 3 using eq 7 for the dielectric function of the silver particles.

Accordingly, we amended the free electron dielectric function to include Lorentzian oscillators that classically represent the interband transitions experienced by bound electrons in the metal. The optical properties of bulk materials such as MgO as well as yttrium nanoparticle systems have been successfully modeled using this form of the dielectric function.[1,24] We found that the experimental data could be represented using two Lorentzian oscillators along with the Drude terms for the silver particle dielectric function.

$$\epsilon = 1 - \frac{\omega_p^2}{\omega^2 + i\gamma\omega} + \sum_{j=1}^{2} \frac{a_j^2}{\omega_{0j}^2 - \omega^2 - i\omega\Gamma_j} + \epsilon_\infty \quad (7)$$

where the first two terms correspond to the Drude free electron model and the third term is a summation of two Lorentzian oscillators. In the Lorentz term, a_j is an oscillator strength, ϵ_∞ is the dielectric function of the metal in the high-frequency limit, and ω_{0j} and l_j are the resonant frequencies and damping constants, respectively. This form of the dielectric function conforms to the requirements of the Kramers−Kronig relation.[25]

4. Results and Discussion

Extinction data were modeled using eqs 3 and 7 and compared to the model using a least-squares fitting routine, letting *f*, ϵ_m, a_j, ω_{0j}, l_j, ϵ_∞, ω_p, ,and γ vary. The best fit to the experimental data is shown in Figure 6. The choice of two oscillators appears obvious, as there are two features that dominate the absorption spectrum at wavelengths below that of the SPR at ~392 nm.

These results can be compared to those obtained by Moskovits et al., who made use of a model including three Lorentz-type oscillators,[25] the third ostensibly to fit an irregularly shaped minimum near 300 nm in their data. Our sample shows symmetric features that are fit quite well using only two oscillators in our model. This perhaps reflects the purity of our samples since the evacuated free volume in the fluoropolymer matrix provides an isolated, chemically inert environment for particle synthesis, furthering the idea that the lower wavelength features are due to bound electron contributions and are not related to contaminants.

While the TEM images give us good estimates for particle size and provide some information on particle distribution, we are not able to definitively determine particle shapes for our composites. A variety of particle shapes for silver nanoparticles have been reported in the literature that appear to depend on a number of processing conditions. On the basis of considerations

TABLE 1: Extracted Parameters for Best Fit of Eq 3 to the Measured Absorption Spectrum of 1× Silver−FEP Material Using Eq 7 as the Dielectric Function of the Silver Particles

f	ϵ_m	a_1 (eV)	a_2 (eV)	ω_{01} (eV)	ω_{02} (eV)	Γ_1 (eV)	Γ_2 (eV)	ϵ_∞	ω_p (eV)	γ (eV)
3.29×10^{-5}	1.596	−5.64	−2.65	5.299	3.959	1.987	0.465	1.102	8.973	0.082

of our synthesis process, the silver particles could be spherical, cubic, or octahedral solids, but no definite assignment based on our characterization can be made at this time. It should be noted that attempts were made to model the experimental results using particles both as spheres with no interband transitions and also as cubic particles with no interband transitions. The spherical model without interband effects was able to reproduce the surface plasmon peak, however, and did not account for the interband features. We also attempted to use the cubic model derived by Fuchs[26] that accounts for six dominant absorption modes due to the faceted nature of the cube. We found it was not possible to fit the measured spectrum using this model because the lower wavelength features in our spectrum could not be fit by the resonances of the cube. In addition, we believe that the majority of the particles are spherical since it has been shown that increased faceting of silver nanoparticles leads to a red shift of the surface plasmon peak[27,28]—the 1× composite SPR peak resides in the region expected for spherical silver particles. These results taken together convinced us of the appropriateness of using the Maxwell−Garnett model to describe our system.

While the model we have used here contains a significant number of adjustable parameters that are varied to fit our data, it was found that the minimization function had a great number of local maxima and minima that precluded an acceptable fit of the model to the data based on arbitrary assignment of various parameters. On the basis of extensive use of the modeled dielectric function for silver, we believe it can be used to extract physically significant material properties and can be used to understand our material system in ways that accepted, measured dielectric functions cannot. The resulting value for each fitting parameter is given in Table 1. The plasma frequency ω_p is slightly smaller than that calculated for bulk silver. We believe this could be due to the presence of the highly electronegative fluorine atoms in the polymer that constitute much of the particle environment. The presence of these electron-withdrawing atoms attracts free electrons toward the surface of the particle, effectively binding them and leaving fewer free electrons available for conduction processes. By eq 5 a lower number density of free electrons results in a lower plasma frequency. The damping constant extracted here is larger than in studies of silver thin films which is best explained by the reduced mean free path (and hence smaller collision times) provided for electrons in our particles due to their size.[29] Along with contributing to the scattering of conduction electrons, the particle−matrix interface influences the model's value for the matrix dielectric constant. A matrix dielectric constant ϵ_m of 1.596 was obtained, lower than the expected value of 1.727 for FEP but very close to the best value of 1.565 using measured values for the silver dielectric constant. This adjusted value likely stems from the local dielectric constant surrounding the particles differing from uninfused FEP due to involved particle−matrix interface effects.[20] A large contribution to these effects, again, may be due to the particle environment caused by the surrounding fluorine atoms. The interlayer at the metal/matrix interface can differ greatly from that of the native matrix and is likely the origin of the altered value for ϵ_m returned by the model.

The most dramatic result was that the volume fraction from the model was an order of magnitude smaller than the measured volume fraction calculated assuming bulk density. However, as was the case with the matrix dielectric constant, this value of f from the modeled dielectric function was very close to that obtained using the measured bulk silver dielectric function and gave much better agreement than that based on volume fraction analysis. There may be a number of reasons for this discrepancy, but the leading cause might be that only a small percentage of the particles in the matrix dominate the optical absorption. The latter is supported by the fact that larger particles are known to dominate the optical response of metal nanoparticles in the case of a distribution of particle size.[2] It is conceivable that our assumption of a uniform particle size is insufficient and that the majority of the silver present in the FEP matrix is in fact much smaller than the particles that appear prominently in the TEM images.

While the specific details of the electron scattering is beyond the scope of this paper, it is clear that our fluoropolymer matrix along with considerable interband transition contributions affect the unique behavior of the plasmon resonance. The implication is that the silver particles in our 1× material are in a size regime and environment where previously measured bulk dielectric function data are not applicable and variations in the interband transitions must be considered.

5. Conclusion

Silver−FEP nanocomposite materials were synthesized using a novel infusion technique that allows for nucleation of particles inside the polymer matrix. The optical properties of these materials were studied, focusing on the response of the silver nanoparticles from 225 to 600 nm. Prominent features in the absorption spectrum of these materials included peaks related to the surface plasmon resonance and to interband transitions in the silver particles. These peaks were defined most clearly for the composites with the smallest particles—approximately 2 nm radius for the materials in this study. Interband transitions have been modeled for these silver nanoparticles using reported values for the bulk silver dielectric function and by modeling the transitions using classical Lorentz-type oscillators. Attempts to match the absorption spectrum of composites with the smallest silver particles using experimentally derived values of the bulk dielectric function of silver extracted from measurements on both thin films and nanoparticles were unable to reproduce either the experimentally measured SPR peak width or the interband region features. Phenomenological models for the dielectric function of silver were used to reproduce the absorption spectrum. The interband transitions were modeled by including two Lorentz-type oscillators in addition to the Drude-type terms in the dielectric function. The fit provided excellent agreement with the measured spectrum and returned reasonable values for various optical and physical constants. Two oscillators were shown to be adequate in reproducing the absorption spectrum of the sample with the lowest silver content.

Additional studies will further explore the origin of the accentuated interband behavior of silver nanoparticles in silver−FEP nanocomposites and should give important information on the effects of matrix and particle size on the optical properties of nanoparticle composites.

Acknowledgment. The authors thank Dr. Michael McCaffery at the Integrated Imaging Center at Johns Hopkins

University for assistance with the transmission electron microscopy of the nanocomposites. This work has been supported, wholly or in part, through DARPA Contract MDA972-03-C-0042.

References and Notes

(1) Bohren, C. F.; Huffman, D. R. *Absorption and Scattering of Light by Small Particles*; Wiley: New York, 1983.
(2) Kreibig, U.; Vollmer, M. *Optical Properties of Metal Clusters*; Springer: Berlin, 1995.
(3) Hövel, H.; Fritz, S.; Hilger, A.; Kreibig, U. *Phys. Rev. B* **1993**, *48*, 18178.
(4) Frederix, F.; Friedt, J.; Choi, K.; Laureyn, W.; Campitelli, A.; Mondelaers, D.; Maes, G.; Borghs, G. *Anal. Chem.* **2003**, *75*, 6894.
(5) Lazarides, A. A.; Kelly, K. L.; Jensen, T. R.; Schatz, G. C. *J. Mol. Struct.* **2000**, *529*, 59.
(6) Chatterjee, K.; Banerjee, S.; Chakravorty, D. *Phys. Rev. B* **2002**, *66*, 085421.
(7) Ehrenreich, H.; Philipp, H. R. *Phys. Rev.* **1962**, *128*, 1622.
(8) Marton, J. P.; Jordan, B. D. *Phys. Rev. B* **1977**, *15*, 1719.
(9) Johnson, P. B.; Christy, R. W. *Phys Rev. B* **1972**, *6*, 4370.
(10) Quinten, M. *Z. Phys. B* **1996**, *101*, 211.
(11) Koloski, T. S.; Vargo, T. G. U.S. Patent 5,977, 241, 1999.
(12) Quinten, M. *Appl. Phys. B: Laser Opt.* **2001**, *73*, 317.
(13) He, S.; Yao, J.; Xie, S.; Gao, H.; Pang, S. *J. Phys. D: Appl. Phys.* **2001**, *34*, 3425.
(14) Hammond, C. *The Basics of Crystallography and Diffraction*; Oxford University Press: New York, 1997.
(15) Kreibig, U.; Schmitz, B.; Breuer, H. D. *Phys. Rev. B* **1987**, *36*, 5027.
(16) Ruppin, R. *Phys. Status Solidi B* **1978**, *87*, 619.
(17) Ruppin, R. *J. Appl. Phys.* **1986**, *59*, 1355.
(18) Kreibig, U.; Genzel, L. *Surf. Sci.* **1985**, *156*, 678.
(19) Ashcroft, N. W.; Mermin, N. D. *Solid State Physics*; Thomson Learning: Philadelphia, 1976.
(20) Kreibig, U.; Bour, G.; Hilger, A.; Gartz, M. *Phys. Status Solidi A* **1999**, *175*, 351.
(21) Kreibig, U.; Gartz, M.; Hilger, A.; Neuendorf, R. *Nanostruct. Mater.* **1999**, *11*, 1335.
(22) Kreibig, U.; Fragstein, C. v. *Z. Phys.* **1969**, *224*, 307.
(23) Pinchuk, A.; Kreibig, U.; Hilger, A. *Surf. Sci.* **2004**, *557*, 269.
(24) Gartz, M.; Quinten, M. *Appl. Phys. B: Laser Opt.* **2001**, *73*, 327.
(25) Moskovits, M.; Srnová-Šloufová, I.; Vlčková, B. *J. Chem. Phys.* **2002**, *116*, 10435.
(26) Fuchs, R. *Phys. Rev. B* **1975**, *11*, 1732.
(27) Jin, R.; Cao, Y.; Mirkin, C.; Kelly, K.; Schatz, G.; Zheng, J. *Science* **2001**, *294*, 1901.
(28) Mock, J. J.; Barbic, M.; Smith, D. R.; Schultz, D. A.; Schultz, S. *J. Chem. Phys.* **2002**, *116*, 6755.
(29) Nash, D. J.; Sambles, J. R. *J. Mod. Opt.* **1996**, *43*, 81.